

Provided for non-commercial research and education use.
Not for reproduction, distribution or commercial use.



This article appeared in a journal published by Elsevier. The attached copy is furnished to the author for internal non-commercial research and education use, including for instruction at the authors institution and sharing with colleagues.

Other uses, including reproduction and distribution, or selling or licensing copies, or posting to personal, institutional or third party websites are prohibited.

In most cases authors are permitted to post their version of the article (e.g. in Word or Tex form) to their personal website or institutional repository. Authors requiring further information regarding Elsevier's archiving and manuscript policies are encouraged to visit:

<http://www.elsevier.com/copyright>



ELSEVIER

available at www.sciencedirect.comwww.elsevier.com/locate/scitotenv

Stepwise effects of the BCR sequential chemical extraction procedure on dissolution and metal release from common ferromagnesian clay minerals: A combined solution chemistry and X-ray powder diffraction study

P.C. Ryan^{a,*}, S. Hillier^b, A.J. Wall^c

^aGeology Department, Middlebury College, Middlebury, Vermont 05753 USA

^bMacaulay Institute, Aberdeen, AB15 8QH UK

^cDepartment of Geosciences, Penn State University, University Park, Pennsylvania, 16802 USA

ARTICLE DATA

Article history:

Received 3 July 2008

Received in revised form

11 September 2008

Accepted 12 September 2008

Available online 31 October 2008

Keywords:

Sequential chemical extraction

Trace metal speciation

Soils

Sediments

Chlorite

Smectite

ABSTRACT

Sequential extraction procedures (SEPs) are commonly used to determine speciation of trace metals in soils and sediments. However, the non-selectivity of reagents for targeted phases has remained a lingering concern. Furthermore, potentially reactive phases such as phyllosilicate clay minerals often contain trace metals in structural sites, and their reactivity has not been quantified. Accordingly, the objective of this study is to analyze the behavior of trace metal-bearing clay minerals exposed to the revised BCR 3-step plus aqua regia SEP. Mineral quantification based on stoichiometric analysis and quantitative powder X-ray diffraction (XRD) documents progressive dissolution of chlorite (CCa-2 ripidolite) and two varieties of smectite (SapCa-2 saponite and SWa-1 nontronite) during steps 1–3 of the BCR procedure. In total, 8 (± 1) % of ripidolite, 19 (± 1) % of saponite, and 19 (± 3) % of nontronite (% mineral mass) dissolved during extractions assumed by many researchers to release trace metals from exchange sites, carbonates, hydroxides, sulfides and organic matter. For all three reference clays, release of Ni into solution is correlated with clay dissolution. Hydrolysis of relatively weak Mg–O bonds (362 kJ/mol) during all stages, reduction of Fe(III) during hydroxylamine hydrochloride extraction and oxidation of Fe(II) during hydrogen peroxide extraction are the main reasons for clay mineral dissolution. These findings underscore the need for precise mineral quantification when using SEPs to understand the origin/partitioning of trace metals with solid phases.

© 2008 Elsevier B.V. All rights reserved.

1. Introduction

The toxicity of a given trace metal is largely controlled by speciation, so analysis of metal partitioning, transformation and availability under conditions that represent natural processes (e.g. pH changes, reduction and oxidation) is crucial to understanding metal behavior. Given that heavy metal speciation is primarily a function of the mineralogy and

chemistry of the solid fraction (Tessier et al., 1979), a number of sequential extraction procedures have been applied to the analysis of metal partitioning (Tessier et al., 1979; Quevauviller et al., 1996; Rauret et al., 1999, 2000; Young et al., 2006; Bacon and Davidson, 2008). These methods are based on the premise that chemical compounds of varying strength and reactivity can extract elements from different fractions of the solid phase, which commonly include surface sorption/exchange

* Corresponding author. Geology Department, Middlebury College, Middlebury, Vermont 05753 USA. Tel.: +1 802 443 2557; fax: +1 802 443 2072. E-mail address: pryan@middlebury.edu (P.C. Ryan).

sites, carbonates, the oxidizable fraction (e.g. sulfides and organic matter), the reducible fraction (e.g. hydroxides and some oxides), and a residual fraction that can include less-soluble minerals such as silicates and well-crystalline oxides. Over the past three decades, SEPs have evolved into some of the most common, easily accessible approaches to determining elemental partitioning and trace metal bioavailability in soils and sediments (Young et al., 2006).

Recent articles by Young et al. (2006) and Bacon and Davidson (2008) summarize development and application of extraction schemes. The two most commonly used SEPs are those of Tessier et al. (1979) and the BCR method developed and subsequently revised by the European Commission (Quevauviller et al., 1996; Rauret et al., 1999). The reagents are similar in both approaches. The main difference is that the Tessier scheme was designed to extract elements from specific phases or sites, including (in steps 1–4) exchange sites, carbonates, hydroxides, and sulfides/organic matter. The BCR method was not designed to attack specific phases, but rather to examine the potential for trace metal release under certain environmental conditions (ion exchange, reduction, oxidation), nonetheless it is often assumed that the BCR method will attack the same phases as targeted in the Tessier approach (Young et al., 2006). Silicate minerals are expected to be resistant to Tessier stages 1–4 and BCR stages 1–3, and assumed to be prone to dissolution only during the final-stage strong acid digestion (Young et al., 2006). However, many studies have indicated that the reagents are not as selective as desired and hence SEP results can be compromised by limited understanding of the specificity of the reactants and lack of knowledge regarding the reactivity of many minerals during chemical extraction (Bacon and Davidson 2008). International standardization of protocols and reference standards headed by the BCR of the European Commission has led to improved reliability and precision across laboratories (e.g. Rauret et al., 1999), but questions still persist regarding the response of minerals to various extractants. According to Bacon and Davidson (2008, p. 29), “interpretation of the results of sequential extraction in terms of binding of trace metals to specific minerals is unjustifiable, unless additional, X-ray-based, analytical techniques are applied to the residues at each stage in the extraction to identify precisely the solid components remaining”. Of particular concern are phyllosilicates, many of which are known to be reactive in the presence of extractants commonly used in SEPs (Moore and Reynolds, 1997; Hamer et al., 2003). Some recent studies have sought to address the issue of quantitative mineral analysis associated with SEPs (e.g. Manceau et al., 2004; Scheckel and Ryan, 2004;

Sulkowski and Hirner, 2006), including application of a standard-based quantitative XRD technique to wetland sediment extracted by the BCR SEP which showed that trioctahedral smectite undergoes stepwise dissolution during reduction (HA–HCl) and oxidation (H₂O₂) stages (Ryan et al., 2002). This has important implications for interpretation of sequential extraction results because many investigators assume that no silicate clays dissolve during oxidation and reduction stages, and that those phases that do dissolve in the early stages are poorly crystalline hydroxides, sulfides and organic matter (e.g. Tessier et al., 1979; Young et al., 2006). Given the abundance of clays in many soils and sediments, silicate clay dissolution could significantly impact interpretation of elemental speciation and availability (Manceau et al., 2004), and information regarding silicate clay dissolution during early stages of sequential extractions is essential because trioctahedral clays can contain on the order of 10⁴ mg/kg of trace metals such as Cr, Ni and Zn in octahedral sites (Newman and Brown, 1987). Without accurate mineralogical analysis, trace metals released from such clays could be wrongly attributed to oxides, sulfides or organic matter.

In this study we seek to examine the stability of three Clay Minerals Society (CMS) Source Clays exposed to the BCR standard sequential chemical extraction procedure (Rauret et al., 1999). Our objectives are to quantitatively analyze clay mineral dissolution using quantitative X-ray diffraction (QXRD) of powders combined with analysis of major and trace elements in extracted solutions, and by comparison of mineralogical and chemical data, assess implications for silicate clay dissolution during SEPs. Of the three clays selected for analysis, two are trioctahedral, including an iron (II)-rich chlorite (CCa-2) and a Mg-rich smectite (SapCa-2); the third clay is an Fe(III)-rich dioctahedral smectite (SWa-1). Compositional data for these clays are presented in Table 1. We also carried out the BCR SEP on CRM 483 (Rauret et al., 2000) in order to ascertain experimental precision and to provide mineralogical information for a known reference material.

2. Materials and methods

Materials used in this study are so-called “Special Clays” from the Source Clays Repository of the Clay Minerals Society (<http://www.clays.org/sourceclays/SourceClays.html>), a collection established in 1972 to provide a set of standardized reference clay minerals to the research community. The advantage of studying CMS reference clays is that numerous

Table 1 – Chemical compositions of CMS clays studied herein

	SiO ₂	Al ₂ O ₃	Fe ₂ O ₃	FeO	MgO	CaO	Na ₂ O	K ₂ O	H ₂ O	TiO ₂	Ni	Cr
CCa-2	25.8	18.3	4.1	21.3	20.3	na	na	na	9.0	<0.1	400	800
SapCa-2	51.3	4.42	1.14	<0.1	23.5	1.25	1.14	0.18	16.7	0.09	5	13
SWa-1	47.6	7.69	23.0	0.05	3.32	1.88	<0.15	0.03	17.9	0.54	12	34

na = not analyzed or data not provided.

All results are in wt.% oxides except for Ni and Cr, which are ppm element. Sources of major element data are as follows: CCa-2 ripidolite (Post and Plummer, 1972), SapCa-2 saponite (Post, 1984), SWa-1 nontronite (Clark et al., 1990). Sources of Ni and Cr data are: CCa-2 (Borggaard et al., 1982), SapCa-2 (Newman and Brown, 1987), SWa-1 (Köster et al., 1999).

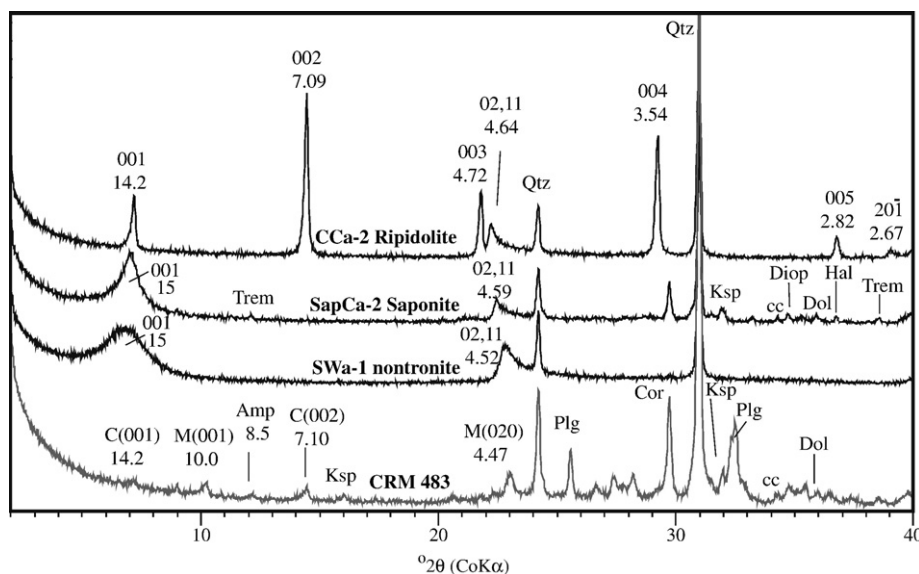


Fig. 1 – XRD data for CMS clays and CRM 483 (<2 mm fraction of each). All are random powder patterns. For clays, d-spacings and hkl data are presented. Mineral abbreviations are as follows: cc = calcite, C = chlorite, Diop = diopside, Dol = dolomite, Hal = halite, Amp = amphibole, Ksp = K-feldspar, M = muscovite, Plg = plagioclase, Qtz = quartz, Trem = tremolite, Cor = corundum. Quartz was added to each CMS clay to assist with tracking of clay dissolution during SEP, and corundum was used to quantify minerals in CRM 483.

experiments have been performed using essentially identical specimens to those studied herein. The minerals selected for this study are as follows:

- Iron(II)-rich trioctahedral chlorite (ripidolite, referenced as CCa-2 in the CMS collection)—formed by hydrothermal alteration of an alpine-type ultramafic body near Flagstaff Hill on the western margin of the Sierra Nevada in California, USA. CCa-2 is a replicate of CCa-1, originally collected and characterized by [Post and Plummer \(1972\)](#).
- Magnesium-rich smectite (saponite, referenced as SapCa-2 in the CMS collection)—found in joints and fracture zones of a metamorphosed dolomite in the Panamint Valley near Ballarat, California, USA. SapCa-2 was originally collected and characterized by [Post \(1984\)](#).
- Iron(III)-rich dioctahedral smectite (nontronite, referenced as SWa-1 in the CMS collection),—formed by weathering of Miocene lava flows in Grant County, Washington, USA ([Clark et al., 1990](#); [Köster et al., 1999](#)).

In order to provide results comparable to other studies on CCa-2, SapCa-2 and SWa-1, specimens were gently ground and the bulk size fraction (sieved to <2 mm) of each reference clay was analyzed in this project. CCa-2 and SWa-1 powders used in this study are free of impurities as demonstrated by XRD analysis. SapCa-2 contains some minor impurities (as demonstrated below, 1% carbonates + halite that are completely removed in Stage 1 of the SEP and 8% non-reactive silicates), but they do not impact the analyses carried out herein ([Fig. 1](#)).

- In addition to the CMS reference clays, the bulk soil (<2 mm) fraction of BCR certified reference material 483 (sewage sludge-applied trace metal-rich soil) was used to gauge

analytical accuracy and recovery, and to assess the effect of sequential extraction on mineral stability in a well-known reference material. Detailed information on collection and preparation of CRM 483 is presented in [Rauret et al. \(2000\)](#).

The three CMS reference clays and CRM 483 were subjected to the revised BCR 3-step plus aqua regia SEP developed by the Standards, Measurements and Testing Programme (formerly BCR) of the European Commission ([Rauret et al., 1999, 2000](#)). All reagents were trace metal grade, and extractions were performed in polypropylene centrifuge bottles. All glassware and containers were cleaned overnight using 1 M HNO₃ and rinsed repeatedly with deionized water. Oven-dried powders were subsampled into 2.4 g aliquots using a sample splitter, and to each 2.4 g aliquot of CMS reference clay, 0.6 g of powdered quartz was added. Given that quartz is resistant to the extractions used in this study ([Clark et al., 2000](#)), it can be used to track clay mineral dissolution, because if clay dissolves, the clay:quartz ratio will decrease. No quartz was added to CRM 483 because it is already sufficiently abundant in this standard (no quartz was detected in the CMS specimens used in this study prior to quartz addition). XRD patterns of pre-extracted powders with quartz added are presented in [Fig. 1](#).

Prior to extraction each sample was oven-dried overnight at 105 °C to drive off adsorbed water ([Rauret et al., 1999](#)), and all results were calculated using oven-dried weights. The reagents used in steps 1–3 of the BCR method of [Rauret et al. \(1999\)](#) plus the aqua regia solution used are presented below, as are solid phases (in parentheses) commonly anticipated to dissolve during each extraction ([Tessier et al., 1979](#); [Young et al., 2006](#)):

1. Exchangeable ions and acid extractable (carbonates)—100 ml of 0.11 M acetic acid (HOAc, pH=3) was applied to each 3.0 g sample. Sample was shaken overnight (16 h) in

Table 2 – Schematic representation of SEP and XRD procedure

ORIG	XRD	HOAc	XRD	HA–HCl	XRD	H ₂ O ₂	XRD	Aq Reg-res	XRD	Aq Reg-fr	XRD
CCa-2-1	XRD	–	–	–	–	–	–	–	–	–	–
CCa-2-2	–	CCa-2-1	→	CCa-2-1	→	CCa-2-1	→	CCa-2-1	XRD	–	–
CCa-2-3	–	CCa-2-2	→	CCa-2-2	→	CCa-2-2	XRD	–	–	–	–
CCa-2-4	–	CCa-2-3	→	CCa-2-3	XRD	–	–	–	–	–	–
CCa-2-5	–	CCa-2-4	XRD	–	–	–	–	–	–	–	–
CCa-2-6	–	–	–	–	–	–	–	–	–	CCa-2-6	XRD

Six sub-specimens were prepared for each specimen. Where “XRD” is indicated, powder was removed after the extraction listed at that stage and analyzed for mineralogical content by XRD. These powders were no longer available for subsequent extractions. An arrow (→) indicates the extracted solution was analyzed for chemical composition and the remaining solids were exposed to the subsequent stage. Although shown only for CCa-2, the same scheme was also applied to SapCa-2, SWa-1 and CRM 483. “Aq Reg-fr” indicates exposure only to aqua regia extraction, and not the previous steps.

an end-over-end shaker at room temperature. Supernatant was separated from the residue by centrifuging at 3000 *g* for 20 min and then filtered through EDTA washed No. 542 filter paper into polypropylene bottles for analysis. Residue was rinsed with Millipore water in an end-over-end shaker and separated by centrifugation.

2. Reducible (Fe–Mn-hydroxides)—100 ml of 0.5 M hydroxylamine hydrochloride (HA–HCl) at pH=1.5 (each 100 ml contained 2.5 ml of 2 M HNO₃) was added to the rinsed, post-HOAc residue, which was processed by shaking, centrifugation and filtration according to the procedure for HOAc.

Table 3 – Sequential extraction data for CMS reference clays

	CCa-2 (Ripidolite)				SapCa-2 (Saponite)				SWa-1 (Nontronite)			
	HOAc	HA–HCl	H ₂ O ₂	AquaRg	HOAc	HA–HCl	H ₂ O ₂	AquaRg	HOAc	HA–HCl	H ₂ O ₂	AquaRg
Ni mg/kg (mean)	36.6	23.9	3.9	132.0	0.38	0.97	0.68	2.67	0.24	1.76	0.65	1.40
Ni std. dev	1.2	0.39	0.29	–	0.12	0.23	0.0	–	0.07	1.5	0.11	–
% total Ni	9.2	6.0	1.0	33.0	7.5	19.4	13.5	53.4	2.0	14.7	5.4	11.7
Cr mg/kg (mean)	5.9	9.5	3.1	102.6	nd	nd	0.78	nd	nd	nd	1.82	3.00
Cr std. dev	0.5	0.7	2.2	–	–	–	0.4	–	–	–	0.4	–
% total Cr	0.7	1.2	0.4	12.8	nd	nd	6.0	nd	nd	nd	5.4	8.8
Si mg/kg (mean)	1211.6	4196.6	172.1	3830.2	1635.9	1762.2	537.6	719.1	1407.0	2852.3	671.4	1104.6
Si std. dev.	14.4	123.9	4.1	–	22.3	15.0	14.4	–	38.0	63.2	40.9	–
% total Si	1.3	4.3	0.2	4.0	0.9	0.9	0.3	0.4	0.7	1.4	0.3	0.5
Al mg/kg (mean)	2415.6	3911.9	447.8	37525.8	52.1	1842.8	1543.9	13326.1	nd	1401.2	3155.4	12112.4
Al std. dev.	43.5	81.1	14.7	–	4.2	23.7	25.8	–	–	32.4	88.4	–
% total Al	3.1	5.0	0.6	48.3	0.3	9.8	8.2	71.2	0.0	4.0	9.0	34.4
Fe mg/kg (mean)	2761.5	7472.4	309.0	68987.0	nd	858.2	24.2	5176.1	nd	5042.2	3008.6	26539.6
Fe std. dev	44.5	111.5	15.8	–	–	16.7	1.1	–	–	71.0	117.1	–
% total Fe	1.8	4.8	0.2	44.3	nd	13.5	0.4	81.1	nd	4.8	2.9	25.2
Mg mg/kg (mean)	2734.4	3213.0	656.1	40178.5	2790.6	12741.0	14678.5	104167	910.4	2147.3	1124.7	4725.7
Mg std. dev	100.4	98.4	7.4	–	36.5	198.7	36.8	–	22.7	43.4	22.1	–
% total Mg	2.8	3.3	0.7	40.9	2.5	11.2	12.9	73.4	6.0	14.1	7.4	31.0
% clay loss-SEP (standard deviation)	2.6 0.7	4.4 1.0	0.5 0.2	44.5 3.7	0.9 1.3	11.5 1.8	7.2 6.3	75.2 5.2	2.0 3.5	7.6 5.6	6.4 3.2	30.2 4.6
% clay loss-XRD (% error)	6.2 4.9	3.0 5	0.0 5	52.3 3.9	3.8 4.9	3.1 5	13.0 4.8	80.1 2.8	4.2 4.9	12.9 4.8	5.7 4.9	21.5 4.6

The first row for each element is mass of that element present in extracted solution, expressed as mg of extracted element per kg of reference clay. The % total depicts the amount of that element extracted at each step relative to the total amount in the reference clay. Standard deviations are determined for 4 replicates for HOAc, 3 replicates for HA–HCl and 2 replicates for H₂O₂ (Table 2). Clay dissolution is represented in two ways: (1) from mineral chemistry calculations based on the averages of Mg, Fe and Al released into solution; and (2) by QXRD data expressed relative to quartz, using quartz as an internal standard and assuming that quartz is stable during the SEP. Bold values represent significant clay dissolution (i.e. greater than % error in QXRD). Note that clay loss is given as % of original clay lost at that specific stage, thus the sum of clay lost at each stage is the total amount of clay lost in the 4 stages of the SEP.

- Oxidizable (sulfides, organic matter)—25 ml of 8.8 M hydrogen peroxide (H_2O_2) was added to each residue and allowed to digest for 1 h with occasional manual mixing. The pH of these solutions was 2.3–2.6. Samples were transferred into a water bath to continue digestion at 85 °C (bottle tops loosened to allow release of pressure) for 1 h after which the bottle caps were removed and samples were allowed to evaporate down to near dryness. This step was repeated. 125 ml of 1 M ammonium acetate (NH_4OAc) adjusted to pH 2 with 2 M HNO_3 was used to extract ions from the residue and procedures were repeated as described in the previous steps.
- Residual (some silicates, well-crystallized oxides)—The aqua regia solution, which consisted of 10 ml (1:1) HNO_3 and 25 ml of (1:4) HCl , was added to each 2.4 g aliquot of residue and placed in a 95 °C water bath for 30 min. Note that this solution (US EPA 200.2) is similar, but not identical, to the one used by Rauret et al. (2000), who used ISO 11466. Samples were filtered and the supernatant was transferred to a 250 ml volumetric flask.

Six 3.0 g sub-samples of each specimen were prepared for analysis. Untreated powders of the three CMS clays and CRM 483 were analyzed by quantitative XRD to determine pre-extraction mineralogical content, and the remaining five sub-samples were analyzed sequentially by SEP and XRD (Table 2). Note that after each step, one sub-sample was removed for XRD and that these specimens were not available for subsequent SEP steps. Solutions were analyzed by inductively coupled plasma-atomic emission spectrometry (ICP-AES) at the Macaulay Institute, and detection limits of elements in solution (mg/L) are as follows: Al (0.8), Ca (0.4), Cd (0.003), Co (0.004), Cr (0.007), Fe (0.1), K (0.1), Mg (0.09), Mn (0.01), Na (0.05), Ni (0.003), P (0.2), Pb (0.02), Si (0.3), Ti (0.01), V (0.004), Zn (0.002). Precision is presented in Table 3 as standard deviations of replicate analyses, and accuracy is assessed in Table 5 by comparison to certified values of Rauret et al. (2000).

Powders were prepared for quantitative XRD analysis by spray drying (Hillier, 1999) to produce random powders for XRD analysis and thereby ensure excellent precision. Spray-dried powders were top-loaded and analyzed in the air-dried state. XRD data were collected on an automated Siemens D-5000 diffractometer with a θ/θ goniometer, Co source, a diffracted beam monochromator, 1° slits, and 0.02° steps with 2 s counts per step. Additional, detailed XRD analyses with 10 s counts were performed on selected powders to enable more precise mineral quantification. Peak intensities for quantitative analysis were determined by measuring integrated areas using Philips X'Pert HighScore software. Unless stated otherwise, expanded uncertainty determined by replicate analysis of standards and using a coverage factor of 2, i.e. 95% confidence, is given by $\pm X^{0.35}$, where X = concentration in wt.%. Using this approach, 5.0 wt.% clay would produce uncertainty of $\pm 1.8\%$, and 75 wt.% clay would produce uncertainty of $\pm 4.5\%$.

Results of mineral dissolution were calculated in two ways. The first was based on concentrations of Al, Mg and Fe in solutions produced during chemical extractions—given that the compositions of CMS reference clays are known (Table 1), mineral dissolution can be determined stoichiometrically from the elemental constituents released into solution. Furthermore, given that there is no interlayer Mg in SapCa-2

(Post, 1984) or SWa-1 (Clark et al., 1990), we can assume that Mg released by SEP is from octahedral sites. Si was not included in compositional calculations for reasons related to SiO_2 saturation at low concentrations in acidic solutions (Langmuir, 1997). The second approach to analyzing mineral dissolution was based on XRD analysis of the ratio of clay content to quartz content. Quartz comprised 20% (wt) of each powder prior to SEP, and assuming that quartz is resistant to dissolution during the SEP (Clark et al., 2000), clay dissolution will be reflected in decreased ratios of clay to quartz. Clay content relative to quartz was quantified by measuring integrated peak areas of 02 and 06 bands for clays and the 100 and 101 peaks for quartz (Fig. 2).

3. Results

As anticipated, all three clay minerals clearly exhibit pronounced dissolution when treated with aqua regia, but each

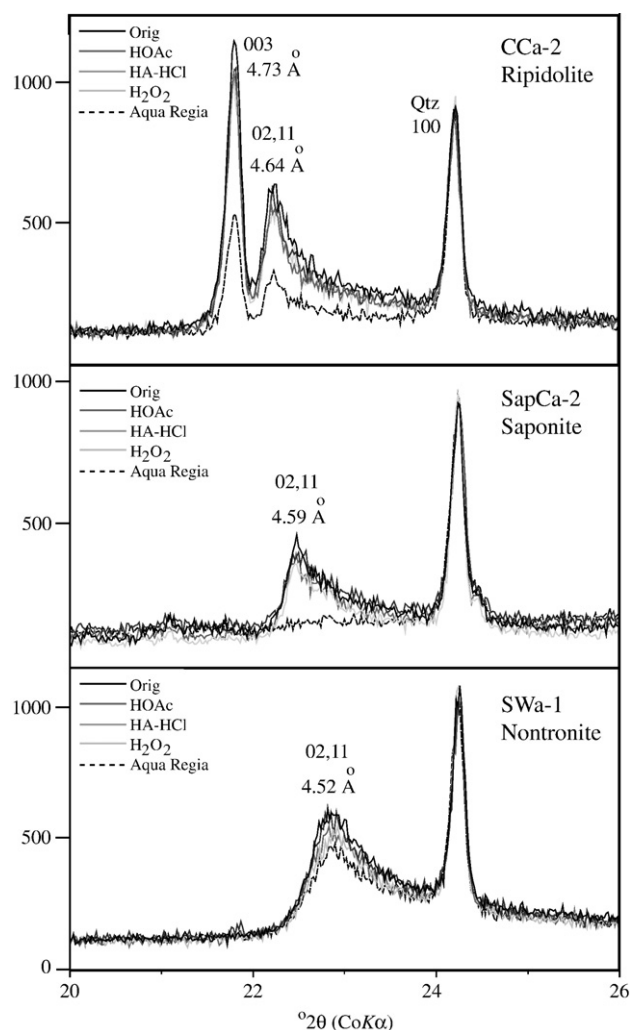


Fig. 2—XRD raw data with evidence for dissolution of clays during SEP. In addition to the quartz 100 peak, the ripidolite 003 peak and 02,11 bands for all three minerals are also shown. Data are from random powder mounts with intensity in counts per second shown on y-axis.

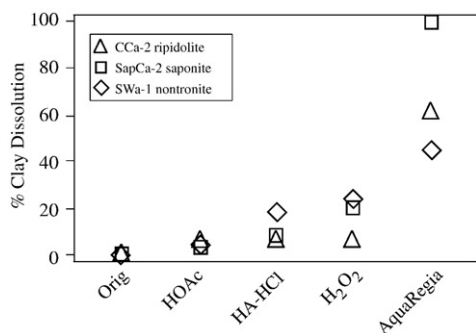


Fig. 3 – Stepwise dissolution of CMS reference clays throughout SEP as determined by XRD. Percent error in XRD-based quantification is encompassed by symbol sizes.

clay also dissolves in smaller amounts during some of the earlier steps frequently assumed to extract carbonates, exchangeable ions, hydroxides, sulfides and organic matter (Table 3; Figs. 2, 3). Most notably, both saponite (SapCa-2) and nontronite (SWa-1) exhibit losses of 3–15% (Table 3) when treated with the reducing agent HA–HCl and the oxidizing agent H₂O₂, based on both quantitative XRD data and stoichiometric calculations from extract compositions. In general, the two approaches to quantifying clay dissolution produce consistent results, with the poorest precision observed in HA–HCl extraction of saponite and H₂O₂ extractions of saponite and nontronite (Table 3; Fig. 4).

3.1. CCa-2 ripidolite

XRD and chemical extract data both indicate small but measurable chlorite dissolution during the first two SEP stages (Fig. 2; Table 3). XRD data indicate dissolution of 6% of CCa-2 during HOAc extraction, while extraction solution stoichiometry indicates loss of 2.6% of the original mass of CCa-2. HA–HCl caused dissolution of a further 3–4% of CCa-2 (3% by XRD; 4.4% by extract stoichiometry), while aqua regia dissolved 44–52% of CCa-2. H₂O₂ caused little or no dissolution of CCa-2 (<0.5%). Approximately 40–50% of CCa-2 remained at the end of the 4-step SEP. Ni extraction generally parallels extraction of Al, Fe and Mg, whereas Cr concentrations are stoichiometrically low in all extracted solutions, perhaps reflecting the relative insolubility of Cr (Brookins, 1988) and its possible re-precipitation as Cr oxide or hydroxide. No mineralogical impurities were detected by XRD analyses of the <2 mm fraction of CCa-2, consistent with previous work of Post and Plummer (1972).

3.2. SapCa-2 saponite

Saponite progressively dissolved throughout the SEP, particularly during H₂O₂, where 10 (±3) % of original saponite dissolved, and aqua regia extraction, where all saponite remaining after the first three stages was destroyed. Compared to H₂O₂, little SapCa-2 dissolved as a result of HOAc and HA–HCl extraction according to XRD (<4% in each stage), although Al–Fe–Mg extraction stoichiometry indicates 11.5% dissolution during HA–HCl (Table 3). While Ni largely parallels the behavior of Al, Fe and Mg, Cr exhibits no correlation with saponite dissolution.

The following mineralogical impurities (quantified by RIR-based QXRD) were identified in the <2 mm fraction of SapCa-2: K-feldspar (4.3%), tremolite (2.5%), diopside (1.3%), dolomite (0.6%), calcite (0.3%) and halite (0.3%). These findings are generally consistent with the findings of Post (1984). XRD data indicate that halite, dolomite and calcite completely dissolved in the first stage (HOAc) while the concentration of the non-clay impurities were not affected by any stage of the SEP. So other than extra Na, Ca and Mg in extract solutions from Stage 1 (HOAc), these impurities do not affect extract chemistry.

3.3. SWa-1 nontronite

Similar to SapCa-2, SWa-1 exhibits significant dissolution (~10%) during H₂O₂ oxidation and notable losses as a result of HA–HCl reduction (10±3%) (Figs. 2, 3). According to XRD and stoichiometric analyses, aqua regia caused dissolution of only 21% of SWa-1 (Table 3). Little or no SWa-1 dissolved as a result of HOAc extraction—losses determined by XRD are less than analytical uncertainty (Table 3) and extract stoichiometry indicates only 1.3% dissolution (Table 3). The release of Ni into solution parallels nontronite dissolution, although in lower percentages than Al, Mg and Fe (of total element in nontronite). No mineralogical impurities were detected by XRD analyses of the <2 mm fraction of SWa-1.

3.4. CRM 483 sediment standard

The mineralogical content and SEP extraction results of CRM 483 are presented in Tables 4 and 5. SEP results demonstrate that mean values for extracts are similar to certified values presented in Rauret et al. (2000) with a few exceptions,

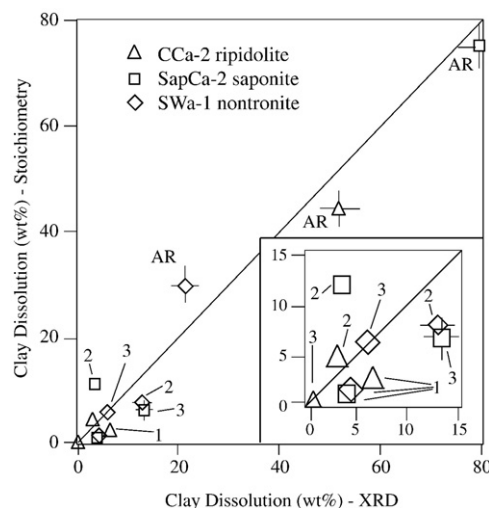


Fig. 4 – Comparison of clay mineral dissolution determined by XRD vs. stoichiometries from SEP solution compositions, for the CMS reference clays. Note that mineral dissolution is given as % clay that dissolved in a given extraction stage, so for SapCa-2, for example, a cumulative 20% of saponite had dissolved by the end of the first 3 SEP stages and the remaining 80% dissolved in aqua regia. Error bars are not given where % error is equal to or less than symbol size. Extraction stages are indicated as follows: 1=HOAc, 2=HA–HCl, 3=H₂O₂, AR=aqua regia. See insert for stages 1–3 detail and Table 3 for data.

Table 4 – Mineralogical content (wt.%) of BCR CRM 483 (<2 mm), ranging from unextracted sediment (Orig) through content after extraction stages to aqua regia (HNO₃-HCl)

Treatment	Qtz	Plag	Ksp	Amp	Cal	Dol	Musc	Chl	Kaol	Sum	% Chl loss
Orig	31.5	19.1	6.8	4.2	1.9	0.5	15.3	4.9	tr	84.2	–
HOAc	35.2	20.0	7.2	3.8	nd	nd	15.2	4.7	tr	86.1	14
HA-HCl	38.1	21.6	7.4	4.4	nd	nd	16.9	4.8	tr	93.2	5
H ₂ O ₂	42.2	23.9	7.9	4.5	nd	nd	17.4	4.3	tr	100.2	16
AquaRegia-res	41.0	24.7	7.7	4.0	nd	nd	16.6	nd	tr	94.0	100
AquaRegia-fr	47.2	25.2	8.9	3.4	nd	nd	13.6	nd	tr	98.3	100

Aqua regia extractions were performed on powders that had been exposed to all stages of the SEP (res) as well as on fresh, unextracted powders (fr). The far right column expresses chlorite dissolution for a given stage normalized to quartz content.

Table 5 – Experimental results for sequential extraction of CRM 483 obtained in this study compared to CRM 483 certified values presented in Rauret et al. (2000)

	Cd	Cr	Ni	Pb	Zn	Al	Ca	Fe	Mg	Si
HOAc, this study	12.1 (0.92)	8.3 (0.6)	19.6 (1.3)	0.31 (.21)	515 (38)	60.7 (1.5)	12399 (722)	51.9 (4.2)	394 (43)	446 (25)
HOAc, certified	10.0 (0.77)	9.4 (3.5)	17.9 (2.0)	0.76 (0.70)	441 (39)	NA	NA	NA	NA	NA
HA-HCl, this study	23.8 (1.0)	662 (20)	21.6 (0.91)	377 (16)	406 (21.5)	2887 (98)	4300 (240)	9629 (423)	149 (9)	631 (72)
HA-HCl, certified	24.8 (2.3)	654 (108)	24.4 (3.3)	379 (21)	438 (56)	NA	NA	NA	NA	NA
H ₂ O ₂ , this study	0.92 (0.03)	1835 (137)	5.3 (0.53)	31.4 (5.6)	30.2 (2.0)	977 (122)	35.3 (21)	970 (192)	201 (31)	128 (65)
H ₂ O ₂ , certified	1.22 (0.48)	2215 (494)	5.9 (1.4)	66.5 (22)	37.1 (9.9)	NA	NA	NA	NA	NA

Results are given with mean and (standard deviation). For this study, N=24 for HOAc, N=15 for HA-HCl, and N=12 for H₂O₂. N=5 for all certified values. Results are in mg/kg. Certified values are not available for major elements.

particularly Pb concentrations from HOAc and H₂O₂, which are lower than certified values (Table 5). Standard deviations of experimental results from this study are generally lower than inter-laboratory certified values. Unextracted CRM 483 sediment consists of quartz (31.5%), plagioclase (19.1%), potassium feldspar (6.8%), amphibole (4.2%), muscovite (15.3%) and chlorite (4.9%) as well as small amounts of calcite (1.9%) and dolomite (0.5%). The mineral sum of 84% implies 16% X-ray amorphous solids, likely dominated by organic matter applied in the form of sewage sludge (Rauret et al., 2000). The sum of the mineral component of CRM 483 is 100% after H₂O₂ extraction, indicating that destruction of organic matter and any other X-ray amorphous material is probably complete

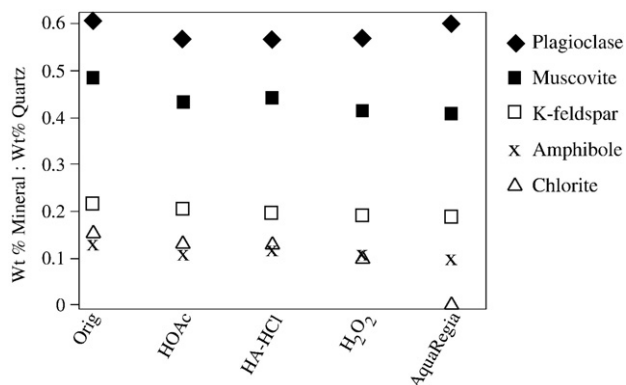


Fig. 5 – Mineralogical content of CRM 483 as a function of sequential extraction stage. Mineral content is expressed relative to quartz, and analytical uncertainty is encompassed by symbol sizes.

following this stage of the SEP. Of observed minerals, only carbonates and chlorite seems to be appreciably affected by SEP. Calcite and dolomite are completely destroyed in the HOAc stage. Aqua regia results in complete chlorite dissolution, H₂O₂ and HOAc each appear to have resulted in dissolution of ~15% of the original chlorite, and HA-HCl about 4% (Fig. 5).

The low concentrations of chlorite make precise quantification difficult, but positive correlation of Mg released by extractions confirms XRD-based observations of chlorite dissolution (Fig. 6). (Destruction of dolomite with HOAc precludes precise correlation of Mg with chlorite XRD data for this extraction stage.) Given that CRM 483 contains high concentrations of sewage sludge-derived trace metals and low chlorite content, we do not observe correlations between chlorite dissolution and trace metals—in other words, due to

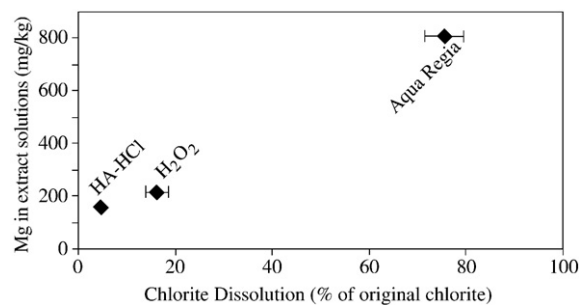


Fig. 6 – Correlation of Mg extracted during SEP vs. XRD-determined dissolution of chlorite in CRM 483. Analytical error for Mg concentrations is encompassed by size of symbols.

the nature of the specimen, the silicate clays in CRM 483 do not exert any notable control on trace metal speciation.

4. Discussion

The results of this study indicate that ferromagnesian chlorite and smectite partially dissolve during HOAc, HA-HCl and H₂O₂ extractions commonly predicted to extract metals bound to exchangeable sites, carbonates, hydroxides, sulfides and organic matter (Tessier et al., 1979; Young et al., 2006). Given the propensity of transition metals like Cr, Ni and Zn to substitute for Mg, Fe and Al in octahedral sheets of phyllosilicates (Newman and Brown, 1987; Manceau et al., 2004), dissolution of phyllosilicates by HOAc, HA-HCl or H₂O₂ could lead to misinterpretation of trace metal speciation when SEPs are applied to phase analysis of clay-bearing soils or sediments. Cr occurs in the octahedral sheet of CCa-2 ripidolite and SWa-1 nontronite, and Ni occurs in the octahedral sheet of all three clays studied herein (Table 1). Concentrations of these metals in extract solutions produced in this study, particularly Ni, are correlated to the extent of clay dissolution (Fig. 7), an observation consistent with metal liberation following destruction of phyllosilicate octahedral sheets.

4.1. Analysis of clay dissolution: XRD vs. extract compositions

Non-stoichiometric dissolution of clays has been noted before, especially with respect to low Si content relative to Al, Fe and Mg (e.g. Ross, 1969; Brandt et al., 2003; Hamer et al., 2003), and many studies have observed destruction of octahedral sheets and preservation of tetrahedral sheets during the breakdown of trioctahedral clays (Ross and Kodama, 1976; Brandt et al., 2003). Solution pH exerts a strong control on Si solubility—Si is highly soluble in alkaline solutions (e.g. 10⁴ mg/L at pH=12) yet

is orders of magnitude less soluble in acidic solutions (Langmuir, 1997). For example, at 20 °C and pH<7, Si in its most soluble form (as amorphous SiO₂) only has a solubility of 50 mg/L (as elemental Si), and considering that aqua regia extracts are allowed to cool to 20 °C before filtration and ICP analysis, it is reasonable to expect similar Si concentrations in aqua regia solutions produced in this study—and in fact, dissolved Si was quite comparable, ranging from 17–92 mg/L Si in post-aqua regia solutions. For comparison, if all Si from chlorite, saponite or nontronite that dissolved during aqua regia extraction were to have gone into and remained in solution, Si concentrations in aqua regia solutions would be on the order of 10³ to 10⁴ mg/L Si. The occurrence of low Si in solution and the formation of amorphous silica in post-extract residues have been noted in acid dissolution experiments on chlorite (Ross, 1969; Ross and Kodama, 1976; Brandt et al., 2003; Hamer et al., 2003), saponite (Suarez Barrios et al., 2001) and nontronite (Stucki et al., 1984).

The general agreement among Al, Fe and Mg concentrations in extract solutions is also consistent with preferential dissolution of octahedral sheets over tetrahedral sheets (Brandt et al., 2003). Concentrations of Al, Fe and Mg in CCa-2 extract solutions are precise and proportional to their concentrations in solid CCa-2 in all 4 stages, and the same is true for Al, Fe and Mg concentrations in saponite and nontronite aqua regia solutions. We do, however, observe varying degrees of non-stoichiometric dissolution of saponite and nontronite in stage 1–3 extractions. In general, Al and Fe are proportionally lower than Mg, which is attributed to buffering of extracted solutions by dissolving clay and low solubility of Al and Fe in circum-neutral solutions relative to Mg (Brookins 1988; Brigatti et al., 1999). This too could affect Cr and other trace metals of relatively low solubility. Similarly, Sulkowski and Hirner (2006) documented buffering-related issues in carbonate-rich soils exposed to the BCR SEP, where dissolving carbonate buffers pH in HOAc solutions.

4.2. Mechanisms of clay dissolution

The presence of ferrous and ferric iron in many silicate clays suggests the potential for oxidation of ferrous iron during H₂O₂ (and possibly also HOAc and aqua regia) extraction and reduction of ferric iron during HA-HCl extraction. In addition to reduction-oxidation reactions, H⁺ attack on mineral surfaces is known to promote hydrolysis of bonds between metal cations and oxygen, resulting in release of these ions into solution (Ross, 1969; Wieland et al., 1988; Kohut and Warren, 2002).

4.2.1. Ripidolite (CCa-2)

Chlorite minerals are generally unstable in acidic environments (Kohut and Warren, 2002). Ripidolite dissolves at 25 °C in weak HOAc (Hamer et al., 2003) and at 20 °C with 0.1 M NaClO₄ (Krawczyk-Bärsch et al., 2004), and in natural settings, chlorite decreases in abundance with increasing soil age (e.g. Bain and Duthie, 1984), in some cases completely dissolving over time spans as little as 60 years in acidic soils turned oxic by wetland draining (Lynn and Whittig, 1966). Other field-based studies (e.g. Bain, 1977) indicate that Fe(II)-rich chlorite is more resistant to the acidic solutions associated with

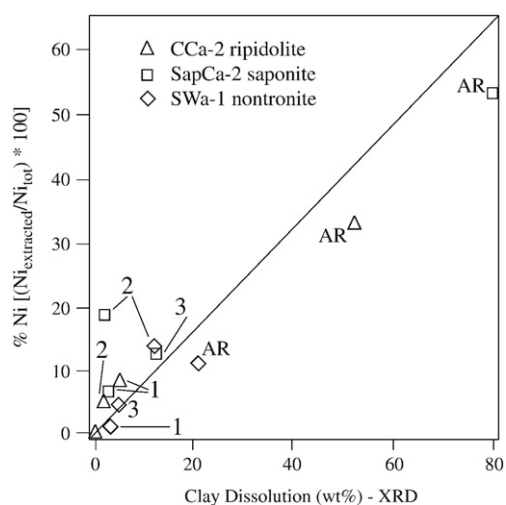


Fig. 7—Correlation of clay mineral dissolution determined by XRD to nickel released during SEP stages, where Ni is expressed as % of Ni extracted in a given stage relative to total Ni in specimens. Symbols are the same as in Fig. 4.

chemical weathering than is Mg-rich chlorite, perhaps due to the fact that the Mg–O bond is weaker than the Fe–O bond in chlorite (362 kJ/mol vs. 409 kJ/mol; Kohut and Warren, 2002). This observation implies that hydrolysis (reaction of H⁺ with metal-oxygen pairs in octahedral sheets) of the octahedral layer is an important control on chlorite decomposition, and may (in addition to saturation of certain elements in solution, particularly Si) explain incomplete ripidolite dissolution during aqua regia extraction.

Chlorite alteration by Fe(II) oxidation has been accomplished in laboratory studies by reaction with Br (Ross and Kodama, 1976; Senkayi et al., 1981) and NaClO₄ (Krawczyk-Bärsch et al., 2004). In soils, chemical weathering of chlorites is driven by oxidation of Fe(II) which leads to destabilization of octahedral layers, in some cases resulting in transformation of chlorite to vermiculite, smectite or related interstratified minerals, and in other cases, complete destruction of chlorite (Bain, 1977; Aspandiar and Eggleton, 2002). Thus, evidence from field and laboratory studies indicates that chlorite is unstable in acidic, oxidizing conditions, and that dissolution is driven by both Fe(II) oxidation and hydrolysis of octahedral metal-oxygen bonds. Dissolution of CCa-2 ripidolite has been observed in the presence of a weak HA–HCl solution (0.25 M, 30 d) that resulted in partial dissolution of CCa-2 driven by reduction of 40% of the Fe(III) in CCa-2 (Jaisi et al., 2007). The data presented in the current study indicate chlorite dissolution in the presence of HOAc, HA–HCl and aqua regia, and the body of existing published research cited above is consistent with chlorite dissolution caused by the combined action of hydrolysis, oxidation and, in the case of HA–HCl, reduction.

4.2.2. Saponite (SapCa-2)

The low concentration of Fe in the saponite analyzed herein (1.1% Fe₂O₃ in SapCa-2; Post, 1984) suggests that dissolution is largely driven by hydrolysis of Mg–O bonds, rather than redox reactions. In fact, SapCa-2 is the only one of the three CMS clays in this study to completely dissolve, an observation consistent with greater hydrolysis-driven destruction due to the predominance in saponite of relatively weak Mg–O bonds (362 kJ/mol) relative to stronger (and more abundant) Fe–O (409 kJ/mol) and Al–O (511 kJ/mol) bonds in ripidolite and nontronite (Newman and Brown, 1987). The dissolution of saponite in dilute acid has been documented, and hydrolysis of octahedral Mg is interpreted as the primary driving force behind dissolution (Brigatti et al., 1999; Suarez Barrios et al., 2001).

4.2.3. Nontronite (SWa-1)

The presence of 23% Fe₂O₃ in SWa-1 nontronite (Clark et al., 1990) implies that reduction of Fe(III) should play a major role in its decomposition, and the dissolution of 10 (±3) % of nontronite during HA–HCl extraction seems to confirm Fe reductive dissolution. Reduction of Fe(III) creates local instabilities in crystal field energies from charge imbalance that can result in nontronite dissolution (Stucki et al., 1984). Octahedral Fe(III) in nontronite is more readily reducible than octahedral Fe(III) in CCa-2 ripidolite (Jaisi et al., 2007), where crystallographic factors that appear to enhance Fe(III) reduction in nontronite include site occupancy (trans-octahedral Fe is more susceptible to reduction than cis-octahedral Fe) and

layer charge (lower layer charge is correlated with greater ease of Fe reduction) (Jaisi et al., 2005). Reduction of octahedral Fe(III) in nontronite has been observed in the presence of various inorganic reagents (Komadel et al., 1995; Jaisi et al., 2007) and microorganisms (Gates et al., 1993), and the dissolution of SWa-1 during the HA–HCl stage is not surprising.

Dissolution of nontronite during H₂O₂ (6% loss), HOAc (2–4% loss), and aqua regia (20–30% loss) extractions is presumably caused by hydrolysis of octahedral Mg–O and Fe–O bonds (Novák and Čičel, 1978; Wieland et al., 1988). The incomplete dissolution of SWa-1 nontronite during aqua regia extraction is attributed to the greater strength of Fe–O bonds and their resistance to hydrolysis relative to weaker Mg–O bonds that dominate the octahedral sheet in saponite (Fig. 8). Resistance to acids is a common trait of dioctahedral clays, whether they are ferric or aluminous (Novák and Čičel, 1978; Moore and Reynolds, 1997).

4.3. Kinetic and compositional effects

Studies of silicate mineral dissolution kinetics emphasize the importance of extractant solution strength, extent of solution saturation, inherent mineral solubilities and exposure time on mineral dissolution (e.g. Wieland et al., 1988; Nagy et al., 1991). For a given SEP, solution strength and exposure time are constant, but mineral dissolution rates vary as a function of composition and structure and thus exert important controls on mineral behavior during SEPs. Experimental data (Novák and Čičel, 1978) reveals that the composition of smectite exerts a strong control on dissolution rate in acid, where magnesian smectites dissolve more rapidly than ferruginous smectites, which in turn dissolve more rapidly than aluminous smectites, reflecting the relative weakness of Mg–O bonds as compared to Fe–O and Al–O bonds. This is consistent with our observation that the magnesian smectite saponite dissolves more completely during the BCR SEP compared to the ferric smectite nontronite and to the Fe–Mg chlorite ripidolite

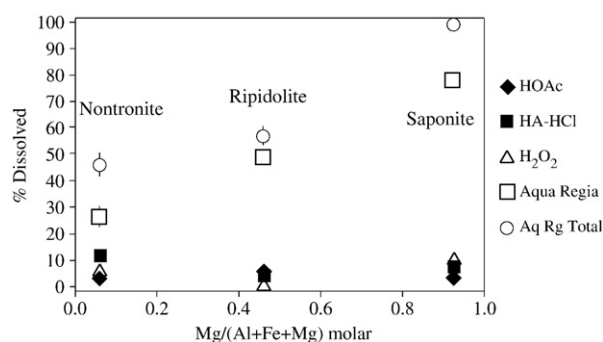


Fig. 8 – Relationship between octahedral sheet composition and clay dissolution during SEP stages. The correlation between octahedral composition and aqua regia dissolution is attributed to greater hydrolysis of relatively weak Mg–O bonds relative to Fe–O and Al–O bonds. Where error bars are not shown, analytical uncertainty is less than symbol size. Data for “Aqua Regia” represent % of original mineral that dissolved during aqua regia following stages 1–3; “Aq Rg Total” signifies dissolution results of specimens exposed only to aqua regia, and not previous steps.

(Fig. 8). Based on bond strengths, aluminous phyllosilicates are predicted to react more slowly in acidic solutions than the clays studied herein.

Numerous studies have demonstrated progressive silicate clay dissolution with time. For example, Senkayi et al. (1981) observed increasing chlorite oxidation with time, and Hamer et al. (2003) note that CCa-2 dissolution increases parabolically with decreasing solution pH (i.e. increasing acidity has a progressively smaller effect on chlorite dissolution rate). Brigatti et al. (1999) noted that saponite exposed to dilute acid in a two-week experiment dissolves parabolically with time, and the majority of dissolution occurs in the first 50 h. Jaisi et al. (2005, 2007) observed parabolic increases in extent of nontronite and ripidolite (CCa-2) dissolution during microbial and chemical Fe(III) reduction with time in both acid (HCl) and chemical reducing agent (HA–HCl), where the greatest amount of dissolution occurs in the earliest stages and then tapers off with time. These observations are consistent with kinetic rate laws describing decreasing dissolution rates with progression of solutions toward saturation (Nagy et al., 1991).

4.4. Trace metal speciation and clay minerals

Understanding the speciation of metals bound to phyllosilicates is crucial in terms of understanding their mobility in natural systems. Trace metals sorbed onto mineral surfaces or in mineral interlayers are far more available for exchange with ambient waters than are metals sequestered in octahedral sites, whose release requires significant mineral dissolution rather than mere exchange. The kinetics of cation exchange are extremely fast and commonly caused by shifts in pore water chemistry, occurring so rapidly that rates are difficult to measure by conventional methods (McBride, 1997). Exchange of interlayer cations can be slower, controlled by particle diffusion out of interlayers as a function of particle size, yet it is still considered a rapid process and interlayer cations are generally considered “environmentally available” (Dähn et al., 2002). The important difference obtained in this study is that stages 1 through 3 of the BCR SEP (and presumably other similar approaches) extract not only the “environmentally available” cations on mineral surfaces and in clay mineral interlayers, but also the less-available octahedral cations sequestered within 1:1 and 2:1 silicate structures (Fig. 9) that are only released by mineral dissolution caused by hydrolysis, reduction and oxidation.

These results should confirm concerns raised by Bacon and Davidson (2008) that SEP stages are not selective of targets such as exchangeable cations, hydroxides or sulfides/organic matter, and that use of SEPs to indirectly determine trace metal associations with mineral phases is fraught with uncertainty. In the absence of quantitative mineral analysis by X-ray or other methods, SEPs should only be applied to determination of the potential for release of metals under environmental conditions (Rauret et al., 1999), which commonly include easily soluble (HOAc), reducible (HA–HCl), oxidizable (H_2O_2) and residual (aqua regia). While rates of hydrolysis, reduction and oxidation of ferromagnesian clays are orders of magnitude slower than ion exchange, these processes do occur in soils and sediments on time scales ranging from tens to thousands of years (Lynn and Whittig, 1966; Bain, 1977; Aspandiar and Eggleton, 2002), thus drawing

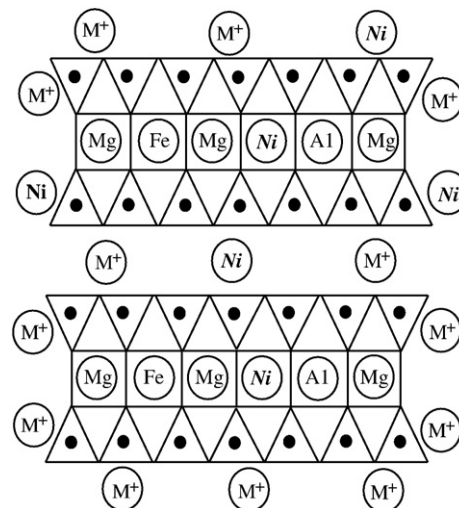


Fig. 9 – Schematic sketch of smectite depicting nickel located in surface exchange sites, in the interlayer, and in octahedral sheets within 2:1 silicate layers. M represents typical exchangeable cations, and the small black circles are Si or Al atoms in tetrahedral sheets.

attention to the potential control exerted by clay minerals on trace metal sequestration and availability. There are numerous examples of clays, particularly smectites, serpentines, and chlorites, with high concentrations of trace metals such as Cr, Ni and Zn (and less frequently Co and Cu) in octahedral sheets (Newman and Brown, 1987), and the literature contains dozens of studies documenting elevated trace metals in clay structures. Studies ranging from Brindley and Maksimovic (1974) to Gaudin et al. (2004) describe Ni-rich layer silicates in various geologic and soil environments, and Oze et al. (2004) report Cr-rich chlorites in serpentine soils. Manceau et al. (2004) describe a natural soil with 128 mg/kg Zn where >80% of the Zn is contained in interlayers and octahedral sheets of magnesian smectite, and Dähn et al. (2002) observed neoformation of Ni-rich smectite layers on montmorillonite surfaces in Ni-rich solutions, further highlighting the effect that silicate clays can exert on metal speciation and sequestration.

5. Conclusions

Ferromagnesian clay minerals exposed to the 3-step BCR plus aqua regia sequential chemical extraction procedure (SEP) progressively dissolve through stages that are often expected to extract metals from structural sites in silicate clay minerals. Our results demonstrate that 8 (± 1) % of CCa-2 ripidolite, 19 (± 1) % of SapCa-2 saponite and 19 (± 3) % of SWa-1 nontronite dissolved during extractions that are often believed to release metals from surface exchange sites, oxyhydroxides, organic matter, and sulfides. Chlorite present in BCR certified reference material CRM 483 exhibited similar behavior. SEPs like the BCR and the Tessier methods are widely-used for the determination of trace metal speciation, yet we know of no prior study that has systematically demonstrated the reactivity of silicate clays during sequential extraction, particularly the behavior of Fe–Mg clays that

commonly contain trace metals such as Cr, Cu, Ni and Zn in octahedral sites. In our experiment, the concentration of Ni in extract solutions is positively correlated with clay dissolution, reflecting liberation of Ni from octahedral sites that are prone to destruction by oxidation, reduction and hydrolysis during the three-step BCR SEP. Relative to stronger Al–O and Fe–O bonds, octahedral Mg–O bonds are particularly vulnerable to hydrolysis in the presence of the weak acids found in all three BCR stages. These results, therefore, call for greater attention to mineralogical analysis of soils and sediments exposed to SEPs in order to avoid ambiguity concerning the identification of sources of trace metals and their availability, especially given the demonstrated reactivity of minerals of the chlorite and smectite groups, which are nearly-ubiquitous in their distribution in soils and sediments.

Acknowledgments

This project was funded by NSF-Hydrological Sciences (EAR 0126018) and the Scottish Government's Rural and Environment Research Directorate. We thank Jeffrey Bacon and two anonymous referees for insightful comments that significantly improved the manuscript, JG Farmer for editorial handling, and Lynne Clark and Martin Wesolowski for assistance in the laboratory.

REFERENCES

- Aspandiar MF, Eggleton RA. Weathering of chlorite: I. Reactions and products in microsystems controlled by the primary mineral. *Clays Clay Miner* 2002;50:685–98.
- Bacon JR, Davidson CM. Is there a future for sequential chemical extraction? *Analyst* 2008;133:25–46.
- Bain DC. The weathering of chloritic minerals in some Scottish soils. *J Soil Sci* 1977;28:144–64.
- Bain DC, Duthie DML. The effect of weathering in the silt fractions on the apparent stability of chlorite in Scottish soil clays. *Geoderma* 1984;34:221–7.
- Borggaard OK, Lindgreen HB, Mørup S. Oxidation and reduction of structural iron in chlorite at 480 °C. *Clays Clay Miner* 1982;30:353–64.
- Brindley GW, Maksimovic Z. The nature and nomenclature of hydrous nickel-containing silicates. *Clay Miner* 1974;10:271–7.
- Brandt F, Bosbach D, Krawczyk-Bärsch E, Arnold T, Bernhard G. Chlorite dissolution in the acid pH-range: a combined microscopic and macroscopic approach. *Geochim Cosmochim Acta* 2003;67:1451–61.
- Brigatti MF, Lugli C, Poppi L, Venturelli G. Iron-rich saponite: dissolution reactions and Cr uptake. *Clays Clay Miner* 1999;34:637–45.
- Brookins DG. Eh–pH diagrams for geochemistry. Berlin: Springer-Verlag; 1988. 176 pp.
- Clark MW, Davies-McConchie F, McConchie D, Birch GF. Selective chemical extraction and grain size normalisation for environmental assessment of anoxic sediments: validation of an integrated procedure. *Sci Total Environ* 2000;258:149–70.
- Clark RN, King TVV, Klejwa M, Swayze G, Vergo N. High spectral resolution reflectance spectroscopy of minerals. *J Geophys Res* 1990;95:12653–80.
- Dähn R, Scheidegger AM, Manceau A, Schlegel ML, Baeyens B, Bradbury MH, et al. Neoformation of Ni phyllosilicate upon Ni uptake on montmorillonite: a kinetics study by powder and polarized extended X-ray absorption fine structure spectroscopy. *Geochim Cosmochim Acta* 2002;66:2335–47.
- Gates WP, Wilkinson HT, Stucki JW. Swelling properties of microbially reduced ferruginous smectite. *Clays Clay Miner* 1993;41:360–4.
- Gaudin A, Petit S, Rose J, Martin F, Decarreau A, Noack Y, et al. Accurate crystal chemistry of ferric smectites from the lateritic nickel ore of Murrin Murrin (Western Australia); I, XRD and multi-scale chemical approaches. *Clay Miner* 2004;39:301–15.
- Hamer M, Graham RC, Amrhein C, Bozhilov KN. Dissolution of ripidolite (Mg, Fe-chlorite) in organic and inorganic acid solutions. *Soil Sci Soc Am J* 2003;67:654–61.
- Hillier S. Use of an air-brush to spray dry specimens for X-ray powder diffraction. *Clay Miner* 1999;34:127–35.
- Jaisi DP, Kukkadapu RK, Eberl DD, Dong H. Control of Fe(III) site occupancy on the rate and extent of microbial reduction of Fe(III) in nontronite. *Geochim Cosmochim Acta* 2005;69:5429–40.
- Jaisi DP, Dong H, Liu C. Influence of biogenic Fe(II) on the extent of microbial reduction of Fe(III) in clay minerals nontronite, illite, and chlorite. *Geochim Cosmochim Acta* 2007;71:1145–58.
- Kohut CK, Warren JC. Chlorites. In: Ammonette, JE, Bleam, WF, Schulze, DG, Dixon, JB, editors. *Soil mineralogy with environmental applications*; 2002. p. 531–54. Soil Science Society of America Book Series No.7.
- Komadel P, Madejova J, Stucki JW. Reduction and reoxidation of nontronite: questions of reversibility. *Clays Clay Miner* 1995;43:105–10.
- Köster HM, Ehrlicher U, Gilg HA, Jordan R, Murad E, Onnich K. Mineralogical and chemical characteristics of five nontronites and Fe-rich smectites. *Clay Miner* 1999;34:579–99.
- Krawczyk-Bärsch E, Arnold T, Reuther H, Brandt F, Bosbach D, Bernhard G. Formation of secondary Fe-oxyhydroxide phases during the dissolution of chlorite—effects on uranium sorption. *Appl Geochem* 2004;19:1403–12.
- Langmuir D. *Aqueous environmental geochemistry*. Upper Saddle River, New Jersey: Prentice-Hall; 1997. 600 pp.
- Lynn WC, Whittig LD. Alteration and formation of clay minerals during cat clay development. *Clays Clay Miner* 1966;14:241–8.
- McBride MB. *Environmental chemistry of soils*. New York: Oxford Univ Press; 1997. 406 pp.
- Manceau A, Marcus MA, Tamura N, Proux O, Geoffroy N, Lanson B. Natural speciation of Zn at the micrometer scale in a clayey soil using X-ray fluorescence, absorption, and diffraction. *Geochim Cosmochim Acta* 2004;68:2467–83.
- Moore DM, Reynolds Jr RC. *X-ray diffraction and the identification and analysis of clay minerals*. New York: Oxford Univ. Press; 1997. New York, 378 pp.
- Nagy KL, Blum AE, Lasaga AC. Dissolution and precipitation kinetics of kaolinite at 80 °C and pH 3: the dependence on solution saturation state. *Am J Sci* 1991;291:649–86.
- Newman ACD, Brown G. The chemical constitution of clays. In: Newman, ACD, editor. *The chemistry of clays and clay minerals*. London: Mineralogical Society; 1987. p. 1–128.
- Novák I, Čičel B. Dissolution of smectites in hydrochloric acid: II. Dissolution rate as a function of crystallochemical composition. *Clays Clay Miner* 1978;26:341–4.
- Oze C, Fendorf SE, Bird DK, Coleman R. Chromium geochemistry in serpentinized ultramafic rocks and serpentine soils in the Franciscan Complex of California. *Am J Sci* 2004;304:67–101.
- Post JL. Saponite near Ballarat, California. *Clays Clay Miner* 1984;32:147–53.
- Post JL, Plummer CC. The chlorite series of Flagstaff Hill area, California: a preliminary investigation. *Clays Clay Miner* 1972;20:271–83.
- Quevauviller Ph, van der Sloot HA, Ure A, Muntau H, Gomez A, Rauret G. Conclusions of the workshop: harmonization of leaching/extraction tests for environmental risk assessment. *Sci Total Environ* 1996;178:133–9.

- Rauret G, López-Sánchez JF, Sahuquillo A, Rubio R, Ure AM, Davidson CM, et al. Improvement of the BCR three step sequential extraction procedure prior to the certification of new sediment and soil reference materials. *J Environ Monit* 1999;1:57–61.
- Rauret G, López-Sánchez JF, Sahuquillo A, Ure AM, Davidson CM, Gomez A, et al. Application of a modified BCR sequential extraction (three-step) procedure for the determination of extractable trace metal contents in a sewage sludge amended soil reference material (CRM 483), complemented by a three-year stability study of acetic acid and EDTA extractable metal content. *J Environ Monit* 2000;2:228–33.
- Ross GJ. Acid dissolution of chlorites: Release of magnesium, iron and aluminum and mode of acid attack. *Clays Clay Miner* 1969;17:347–54.
- Ross GJ, Kodama H. Experimental alteration of a chlorite into a regularly interstratified chlorite-vermiculite by chemical oxidation. *Clays Clay Miner* 1976;24:183–90.
- Ryan PC, Wall AJ, Hillier SJ, Clark L. Insights into sequential chemical extraction procedures from quantitative XRD: a study of trace metal partitioning in sediments related to frog malformities. *Chem Geol* 2002;184:337–57.
- Scheckel KG, Ryan JA. Spectroscopic speciation and quantification of lead in phosphate-amended soils. *J Environ Qual* 2004;33:1288–95.
- Senkayi AL, Dixon JB, Hossner LR. Transformation of chlorite to smectite through regularly interstratified intermediates. *Soil Sci Soc Am J* 1981;45:650–6.
- Stucki JW, Golden DC, Roth CB. Effects of reduction and reoxidation of structural iron on the surface charge and dissolution of dioctahedral smectites. *Clays Clay Miner* 1984;32:350–6.
- Suarez Barrios M, de Santiago Buey C, Garcia Romero E, Martin Pozas JM. Textural and structural modifications of saponite from Cerro del Aguila by acid treatment. *Clay Miner* 2001;36:483–8.
- Sulkowski M, Hirner AV. Element fractionation by sequential extraction in a soil with high carbonate content. *Appl Geochem* 2006;21:16–28.
- Tessier A, Campbell PGC, Bisson M. Sequential extraction procedure for the speciation of particulate trace metals. *Anal Chem* 1979;51:844–51.
- Wieland E, Wehrli B, Stumm W. The coordination chemistry of weathering. III. A generalization on the dissolution rates of minerals. *Geochim Cosmochim Acta* 1988;52:1969–81.
- Young SD, Zhang H, Tye AM, Maxted A, Thums C, Thornton I. Characterizing the availability of metals in contaminated soils. I. The solid phase: sequential extraction and isotopic dilution. *Soil Use Manage* 2006;21:450–8.